

Long-tail Visual Relationship Recognition with a Visiolinguistic Hubless Loss

Sherif Abdelkarim^{1*}, Panos Achlioptas², Jiaji Huang³, Boyang Li⁴,
Kenneth Church³, Mohamed Elhoseiny^{1,2*}

¹King Abdullah University of Science and Technology ²Stanford University

³Baidu Research ⁴Nanyang Technological University

sherif.abdelkarim91@gmail.com*, panos@cs.stanford.edu, huangjiaji@baidu.com,
lily.liboyang@ntu.edu.sg, kennethchurch@baidu.com, mohamed.elhoseiny@kaust.edu.sa*

Abstract. Scaling up the vocabulary and complexity of current visual understanding systems is necessary to bridge the gap between human and machine visual intelligence. However, a crucial impediment to this end lies in the difficulty of generalizing to data distributions that come from real-world scenarios. Typically such distributions follow Zipf’s law which states that only a small portion of the collected object classes will have abundant examples (head); while most classes will contain just a few (tail). In this paper, we propose to study a novel task concerning the generalization of visual *relationships* that are on the distribution’s *tail*, i.e. we investigate how to help AI systems to better recognize rare relationships like $\langle S:dog, P:riding, O:horse \rangle$, where the subject S, predicate P, and/or the object O come from the tail of the corresponding distributions. To achieve this goal, we first introduce two large-scale visual-relationship detection benchmarks built upon the widely used Visual Genome and GQA datasets. We also propose an intuitive evaluation protocol that gives credit to classifiers who prefer concepts that are *semantically close* to the ground truth class according to wordNet- or word2vec-induced metrics. Finally, we introduce a visiolinguistic version of a Hubless loss which we show experimentally that it consistently encourages classifiers to be more predictive of the tail classes while still being accurate on head classes. Our code and models are available on <http://bit.ly/LTVRR>.

Keywords: long-tail, visual relationships, hubless loss

1 Introduction

Since AlexNet [31] and the ImageNet Large Scale Visual Recognition Challenge [50], the task of visual recognition has witnessed significant progress, often being described as surpassing human performance. However, most existing works make the assumption that training data are abundant, with typically a few hundred to thousands of examples per class [8,31,55,22,24]. A more realistic setup is the

* Corresponding authors

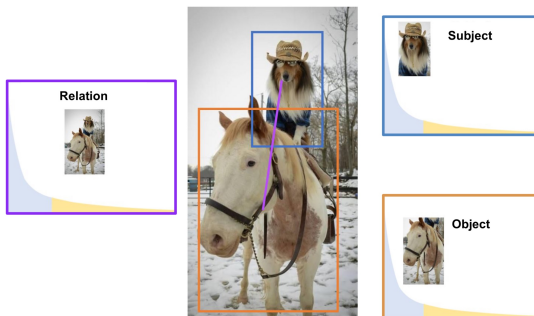


Fig. 1: **Long-Tail Visual Relationship Recognition (LTVRR)**. While dogs and horses occur frequently enough in real-world images, “a dog riding a horse” is a rare occurrence. In *LTVRR* we focus on such rare relational events by introducing i) proper benchmarks, ii) sensitive-to-the-problem evaluation protocols, and iii) well-calibrated losses that can be a *drop-in* replacement to most modern classification systems.

long-tail recognition problem where most categories have only a few examples. While the long-tail distributions have been important in language research for a long time (e.g., [76,77]), the literature on the long tail in vision is relatively recent and less extensive (e.g., [51]). What makes the long tail distribution more natural is that it covers the spectrum of frequent classes, few-shot classes (classes rarely observed in the training set), and even zero-shot classes (classes that do not appear in the training set at all). Few-shot and zero-shot learning has been studied separately in [57,49,71] and [12,13,11,65,65,63], respectively.

Several approaches have been developed to advance long-tail object recognition ([34,36,62,25]). In this paper, we take a step further by bringing this natural long-tail setup to visual relationship recognition. The task is to recognize the categories of two interacting objects and their relation, e.g., recognizing triplets like $\langle \text{dog, riding, horse} \rangle$ [37,44,69]. In our setup, dubbed as *Long-Tail Visual Relationship Recognition (LTVRR)*, relationships, objects and/or subjects follow a long-tail distribution; see Fig 1. In this setup the recognition challenge is exacerbated as the size of the decision space is a multiplication of the number of each of the three elements in the triplet.

Contributions. To the best of our knowledge, we are the first to study the long-tail in a visual relationship detection setting, while also establishing benchmarks to enable studying this problem further. The contributions of this paper are:

- (1) We propose an approach to casting the long-tail understanding as a hubness problem, which to our knowledge is novel. Our approach is inspired from [25], but differs in two aspects: (a) in their work they use the hubness to improve translation from one language to another, while we use hubness in a visio-lingual model where we translate vision to language. (b) The implementation in [25] relies on a provided word embedding and then a translation is proposed to adjust

the embeddings so that hubness is reduced by only tuning biases terms. Our approach can correct learning representation that minimizes hubness from both vision and language sides in an end-to-end fashion. It can also be easily integrated with existing losses like Focal Loss (FL) [34] and Weighted Cross Entropy [34] to improve performance as an effective regularizer.

(2) We propose to use new metrics to analyze different models based on their capacity to bring categories that are semantically similar to the ground-truth, higher in the rank of the model’s predictions, according to six wordNet [39], and word2vec models [70]. We found this to be useful especially when the vocabulary of predictions is large.

(3) We establish a new long-tail VRD benchmark based on GQA dataset [26] and perform several experiments to validate and analyze our setup and compare against the state of the art. We showed that our proposed Visiolingual Hubless Loss improve the performance significantly on the tail classes.

2 Related Work

Visual Relationship Detection Visual relationship detection has been extensively studied in the past few years. Most of the methods used are based on a small vocabulary, e.g., 100 object and 70 relation categories from the VRD dataset [37], or a portion of Visual Genome dataset of the most frequent object and relation categories [68,66].

Lu et.al., proposed one of the first methods [37] which utilize the object detection output of an R-CNN detector and leverage language priors from word embeddings to calibrate the likelihood of a predicted relationship. Zhuang et.al., [75] use language representations of the subject and object as context to improve relation prediction yet still with a pre-trained language representation. Zhang *et al.* [70] allows for the subject and object language representations to be jointly adapted with the visual representation with a two-layer language sub-network on top of language and visual word embeddings. The approach embeds the three relationship components separately to the independent semantic spaces for object and relation, yet learns to fuse the visual features to capture the relationship structure and preserve the semantic meaning in the embedding space. This makes their model more expressive and better performing compared to earlier models including knowledge distillation [67], ViP-CNN [33], and [44]; mainly studied in a much smaller vocabulary.

Semantic Guidance to Zero/Few-Shot Learning The use of word embedding [58] and language for visual embedding has shown promising results especially on recognizing unseen classes from their description; e.g., using word embeddings [17,40] and Attributes / Wikipedia descriptions [14,12,64,32]. Most of the ideas explored in this literature evolved from research on multi-modal vision and language learning, and especially image-sentence retrieval (e.g., [29,60,15,61,19]). Recent work has produced encouraging results on the benefit of using semantic guidance for life-long learning. It is possible to learn new tasks quickly after seeing just a few examples [5]. Looking at these approaches

from a visual relationship recognition angle goes beyond looking at the subject, relations, objects individually, it also models the interaction between objects for visual relations. In regards to the long-tail recognition skill, these results demonstrate the value of using semantic/language embedding for the tail classes and motivates our use of semantic guidance in this paper.

Orthogonal to semantic guidance usage, few-shot learning has also been extensively studied. It is often formulated as meta learning problem [53,2,47,52,16,59]. However, due to the focus on the few-shot classes, they often suffer a significant performance drop for head classes with few recent attempts to alleviate the problem with a forgetting loss on base classes (e.g. [18,48]). The base classes relate in our context to a balanced version of head classes different from few-shot balanced classes; this balancing violates the long-tail distribution assumption.

Long-tail Classification. Long-tail recognition has been extensively studied in the literature [20,7,43,54,6,4,51,73,1,35,74,42]. Early techniques for dealing with skewed label distributions include under-sampling head classes, over-sampling tail classes, and data instance re-weighting; head/tail examples contributes less or more to the training loss. More recent approaches were inspired from *metric learning* [23,41], imposes *hard negative mining* [10,34], *meta learning* [21,62]. A variety of useful learning signals has been proposed including: lifted structure loss [41], range loss [72], focal loss [34]. Focal loss [34] down-weights the loss assigned to well-classified examples which may route the the optimizer to attend more to tail classes which are likely not well classified. Wang et.al. [62] introduced MetaModelNet which learns knowledge head-to-tail transfer model with a meta-regression net that learns to predict good performing classifier from classifiers trained from few-examples from tail categories. Liu et.al, proposed a dynamic meta-embedding meta learning for long-tail recognition [36] that combines the ideas from both metric learning and meta learning. They maintain the dynamic notion by expressing an explicit visual memory model over the centroids of the classes that are allowed to change while maintaining discrimination between categories. The features are adapted with loss in addition to a memory feature produced by an attention layer applied over the learned centroids. However, the work in [28] shows that using decoupling training technique described in their paper surpasses the performance of [36], and that adding the memory module along with the decoupling technique didn't add any improvements to the performance.

In [28], Keng et.al, decouple the representation learning from the balanced classifier learning. They show that best representations are learned when the model is trained without balancing or oversampling the tail classes. While the best classifier is learned when oversampling tail classes. Since different stages of the model require different training conditions, the authors show that it is better to learn them separately instead of jointly. This means the model is trained in two stages. In the first stage, the model is trained where each training sample has the same weighting, meaning no class weighting or balancing. This is stage is where the representation is learned. In the second stage, the representation learned from stage one is frozen, and the classifier of stage one is reinitialized

from scratch. The sampling strategy is also changed so that each class would have the same probability of being sampled. Then the model is trained for an additional number of epochs. They show that learning the model this way is superior to jointly learning the representation and classifier. They also introduce a normalization strategy to apply to the classifier learned in stage one that makes it equivalent to the classifier that would be learned in stage two. This normalization strategy replaces the training in stage two. We perform several experiments using this approach and report the results in Section 5.

3 Background

Hubless Nearest Neighbor (HNN) [25]. A related problem in natural language processing is bilingual lexicon induction where the goal is to translate a word from a language to another. Recent approaches like [46,9,56] have observed that the accuracy of cross-modal retrieval across language is often significantly degraded by a phenomenon called hubness; tendency that a few words (hubs) are too near to too many other words. In long-tail recognition context, this relates to the head which is often over predicted compared to tail classes. Modeling the notion of hubness has led to improved results for tasks like zero-shot learning [9]. Very recently, Huang et.al., [25] proposed an Hubless Nearest Neighbor (HNN) which treats this over prediction problem by imposing an *equal preference* assumption. They modeled the *equal preference* assumption by explicitly encouraging the marginal probability of translating over the target words to be uniform. More concretely, given a dictionary of paired words $\{\mathbf{x}_i, \mathbf{y}_i\}_{i=1}^n$, represented by word vectors (e.g.,[38]), Huang et.al., [25] adds to the standard \mathbf{x}_i a matching \mathbf{y}_i loss. The hubless criterion is defined as

$$\mathcal{L}_{\mathbf{y}}^{Hubless} = pf(\mathbf{y}_i) = \frac{1}{K}, \forall i = 1 \rightarrow K, pf(\mathbf{y}_i) = \frac{1}{N} \sum_{i=1}^N \frac{e^{-\mathcal{D}(\mathbf{x}_i, \mathbf{y}_i)}}{\sum_{j=1}^K e^{-\mathcal{D}(\mathbf{x}_i, \mathbf{y}_j)}} \quad (1)$$

where $\mathcal{D}(\mathbf{x}_i, \mathbf{y}_i)$ measures the distance between a word $\mathbf{x}_i \in \mathcal{X}$ language and a word $\mathbf{y}_i \in \mathcal{Y}$ language. In this context, $\mathcal{D}(\mathbf{x}_i, \mathbf{y}_i)$ is often modeled as $-\mathbf{x}_i^T \mathbf{W} \mathbf{y}_j$. $pf(\mathbf{y}_i)$ is the preference of predicting word \mathbf{y}_i is defined here as the marginalized probability of predicting the \mathbf{y}_i over the entire training examples. The hubless loss encourages this probability to be uniform across the prediction space of the second language \mathcal{Y} . In our work, we develop a vision & language deep-learning approach that is based on the linear approach in [25] that only correct biases parameters. In our work, we alleviate the hubness problem by correcting both the language and visual representations in an end-to-end manner. To our knowledge we are the first to develop this idea into a structured visiolingual understanding problem such as visual relationship understanding to benefit the tail classes.

4 Approach

Given an image, a visual embedding sub-networks processes the image to output three visual embeddings x^s, x^p , and x^o for subject, relation, and object.

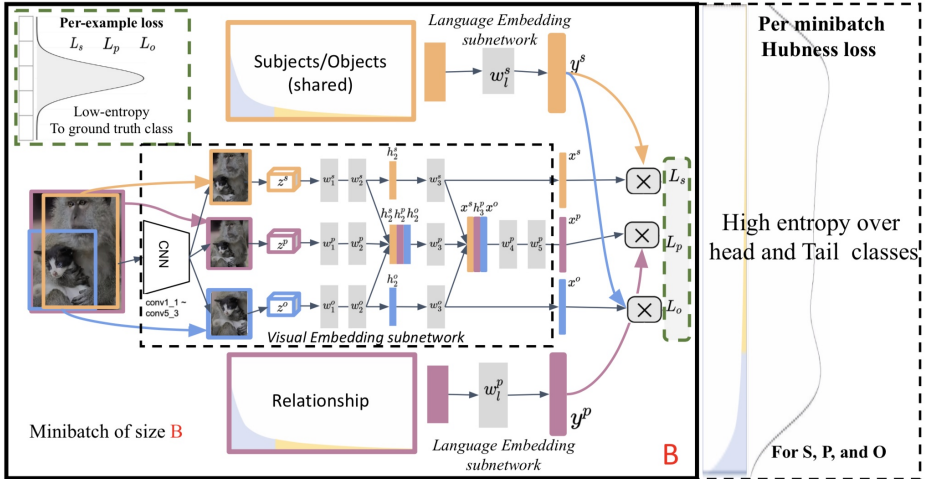


Fig. 2: **Main proposed architecture.** Our model is inspired from [70] and it consists of a Visual Embedding Network and a Language Embedding Network. L_s, L_p, L_o are per-example losses of subject, relation and object denoted here as *low-entropy losses*. Orange, purple and blue colors represent subject, relation, object, respectively. The layer weights of the subject and object branches are shared, *i.e.* w_i^s and $w_i^o, i = 1, 2, \dots, 5$.

Similarly, we represent class labels for subject, relation, object by word embeddings that are fed into language embedding sub-network that outputs three semantic embeddings y^s, y^p, y^o . During training, the standard practice is to align visual and semantic embeddings of matching labels using a loss function. This approach has been comprehensively studied orthogonal to the long-tail context (e.g., [17,40,15]). We build on top one of the best performing losses, dubbed Triplet Softmax loss [70,45] which inherits the discriminative power of Softmax MCE loss and integrates to better align visual and semantic embeddings. However, long-tail distribution was less explored in visual relationship detection. We propose to model the long-tail prediction as a hubness problem [46,9,56,25] inspired from recent progress in natural language processing as we discussed in Sec 3. The key idea for the hubness inspired approach is to encourage fair prediction on both the head and the tail; see Fig 2. Inspired from the plate notation used in Latent Dirichlet allocation [3], we look at the minibatch processing of visual relationships as Plate that we use to approximate fair prediction on head and tail classes. More explicitly, marginalize the predictive preference over each class in each minibatch of size B and we encourage them to be entropic (equally preferred). This applies to a shared prediction space for subjects and objects and a separate space for relationships. During testing we feed word vectors of all objects and relations and use nearest neighbor searching to predict relationship triplet labels. We present the details of our approach in the following subsections.

Visual and Language Subnetworks. Similar to [44,70], we learn embeddings for subject and object in a separate semantic space from the relation space;

see the visual-embedding sub-network in the middle of Fig 2. The subject and object branch have shared weights. On the language side, we feed word vectors of subject, relation and object labels into a neural network with two *fc* layers which outputs the final embeddings. Similar to the visual module, the subject and object branches share weights while the relation branch is learned separately; see Fig 2 top and bottom parts.

Language and Visual Context Word Embeddings. The language sub-network takes as an input Skip-gram word Embeddings, which tries to maximize classification of a word based on another word in the same context. We performed experiments with two skip-gram models trained on language and visual contexts. The language word embedding model is provided by word2vec [38], pre-trained on Google News corpus as context. The second *visual word embedding model* is trained with the same loss of a skip-gram word2vec model where the context is defined as the training relationship instances. The optimization maximizes the likelihoods of each relationship element given the other two (e.g., each of S, P, and O given SO, PO, SP, respectively).

4.1 Hubless Triplet Softmax Loss

Given a set of each positive visual-language pair by $(\mathbf{x}^l, \mathbf{y}^l)$ represented by the aforementioned neural network, joint vision-language embeddings can be achieved by a traditional triplet loss (e.g., [29,60,15]). The triplet loss encourages matched embeddings from the paired modalities to be closer than the mismatched ones by a margin m . Formally, we denote a triplet $tri_{\mathbf{y}}^l = \{\mathbf{x}^l, \mathbf{y}^l, \mathbf{y}^{l-}\}$ where $l \in \{s, p, o\}$ with negatives from the language space. Omitting the superscripts $\{s, p, o\}$ for simplicity, the triplet loss \mathcal{L}^{Tr} for each branch is defined as:

$$\mathcal{L}_y^{Tr} = \frac{1}{NK} \sum_{i=1}^N \sum_{j=1}^K \max[0, m + \mathbf{x}_i^{\top} \mathbf{y}_{ij}^- - \mathbf{x}_i^{\top} \mathbf{y}_i] \quad (2)$$

where N is the number of positive ROIs, K is the number of negative samples *per positive* ROI, m is the margin between the distances of positive and negative pairs. The triplet loss however, does not sense a learning signal beyond the margin and the trained model will not learn to distinguish different classes enough for a classification-oriented task. To alleviate this problem, Zhang et.al. [70] recently studied a Softmaxed version of the triplet loss for visual relationship recognition achieving state of the art results. Triplet Softmax loss can be defined as follows:

$$\mathcal{L}^{TrSm} = \frac{1}{N} \sum_{i=1}^N -\log \left(p_i = \frac{e^{\mathbf{x}_i^{\top} \mathbf{y}_i}}{e^{\mathbf{x}_i^{\top} \mathbf{y}_i} + \sum_{j=1}^K e^{\mathbf{x}_i^{\top} \mathbf{y}_{ij}^-}} \right) = \frac{1}{N} \sum_{i=1}^N -\log \left(p_i = \frac{e^{\mathbf{x}_i^{\top} \mathbf{y}_i}}{\sum_{j=1}^K e^{\mathbf{x}_i^{\top} \mathbf{y}_j}} \right) \quad (3)$$

For each positive pair $(\mathbf{x}_i, \mathbf{y}_i)$ and its corresponding set of negative pairs $(\mathbf{x}_i, \mathbf{y}_{ij}^-)$, the similarities between each of them is computed with dot product and then

put into a softmax layer followed by multi-class logistic loss so that the similarity of positive pairs would be pushed to be 1, and 0 otherwise. In the second line of Eq 3, we show that triplet softmax can be simplified in a form that is very similar to MCE loss if all the other classes except the ground truth are considered negative; see Eq.1 in Sec. 3. We adopted a weighted version of this visiolingual loss where we allow each class to have a weight w_i , so this weight can be assigned to higher values for less frequent classes (e.g., inverse the frequency of the object/relationship class); see Eq. 4.

$$\mathcal{L}_w^{TrSm} = \frac{1}{N} \sum_{i=1}^N -w_i \log \left(p_i = \frac{e^{\mathbf{x}_i^\top \mathbf{y}_i}}{\sum_{j=1}^K e^{\mathbf{x}_i^\top \mathbf{y}_j}} \right) \quad (4)$$

Our Final Loss. Representing joint-semantic embedding loss in Triplet Softmaxed form does only more discriminative joint-embedding model but also it makes them easier to integrate with our hubless loss that is inspired by [25]. The key idea of our approach is to encourage fair prediction over both head and tail classes. In conclusion, our final loss is

$$\mathcal{L} = \mathcal{L}_w^{TrSm} + \lambda \mathcal{L}_h^{TrSm}, \mathcal{L}_h^{TrSm} = \sum_{i=1}^K \left(pf(\mathbf{y}_i) - \frac{1}{K} \right)^2, pf(\mathbf{y}_i) = \frac{1}{B} \sum_{i=1}^B \frac{e^{\mathbf{x}_i^\top \mathbf{y}_j}}{\sum_{j=1}^K e^{\mathbf{x}_i^\top \mathbf{y}_j}} \quad (5)$$

where B is the batch size and α is the hubness strength. The first term \mathcal{L}_w^{TrSm} encourage the examples to be discriminatively classified correctly in the visual-language space. The second term, hubness alleviation loss \mathcal{L}_h^{TrSm} encourages the all the classes (head and tail) to be equally preferred, inspired by [25]. To achieve this behavior, we define the preference of every class as $pf(\mathbf{y}_i)$ as the average probability of the class being predicted in the current minibatch of size B . Then, we simply encourage this probability to be close to uniform (i.e., equally preferred across head and tail). Note that this form allows us to explore other loss function including the focal loss [34] to our LTVRR problem but we found that our hubless triplet softmax loss performing the best in our experiments .

5 Experiments

5.1 Datasets

We present experiments on two datasets, a smaller version of *Visual Genome* (dubbed VG8k)[30,70], and GQA dataset [26] since both are naturally long-tail in their relationships covering subjects, predicates, and objects.

GQA [26]. We used the visual relationship notations provided with the GQA dataset which we found following a long-tail distribution. The main filtration we applied to GQA data was to remove the objects that did not belong to a subject-relation-object triplet, because our main focus is visual relationship detection, not object detection. The resulting dataset had 72, 580 training images

and 10,295 testing images, with 1,703 objects and 310 relations. We split the test set into 7,722 test images and 2,573 validation images.

VG8k [30,70]. We use the latest version of Visual Genome (VG v1.4) [30] that contains 108,077 images with 21 relationships on average per image. We use the data split in [70] which has 103,077 training images and 5,000 testing images following [27] and used the class labels that have corresponding word embeddings [38]. We did some additional filtration on the dataset and based on frequency-based criteria we selected 5,330 classes out of the original 53,304 categories and 2,000 relationships out of the original 29,086 to make a smaller version of VG80K. We call this version VG8k. The resulting dataset has 99,622 training images, and 4,860 testing images. We split the training set into 97,623 training images and 1,999 validation images. Images of the least frequent object and predicate classes are 14 and 18 respectively, meaning the distribution is still very long-tailed.

5.2 Comparison Models.

We compare our method with several state-of-the-art approaches [70,34,28]. We further perform ablation studies on our *mini-batch level* hubless loss on how it can improve the performance when it is integrated with existing example-level losses. Note that all the models use the same learning representation for fair comparisons in our experiments.

Baseline [70]: this is the visio-lingual model used in [70].

Focal Loss (FL) [34]: we tried using the same model in [70] but add focal loss (with varying gamma values) to see how much it would help performance on the tail.

Weighted Cross Entropy (WCE) : In this model we use the loss in [70] but use a standard weighted cross-entropy instead of standard cross-entropy. The weight is based on the inverse class frequency, which gives a large weight to rare classes and a small weight to common classes.

Fully Connected (FC): Here we remove the language guidance part of [70] and replace it with 1 fully connected layer. We use this as a baseline to compare the decoupling models [28] against.

Decoupling (DCPL) [28]: As the time of writing this paper, this is the state of the art in long-tail classification problem. We included this baseline to test whether the same improvements observed in the classification problem would transfer to visual relationship recognition and to compare it against our suggested model. We implemented two versions of the decoupling model. The first version is the same setup described here [28] as the τ -normalized classifier. Following the training procedure in [28], we first train the fully connected version (described above) until convergence. Then we do the normalization strategy suggested in their work with different values of τ to the classifier layer, we refer to this version as DCPL $_{\tau}$. For the second version, we modify their setup to better work for our problem. Instead of training the model using an FC layer as a classifier and then normalize it, we instead use the representation learned from the model trained using the language guidance [70] and add an FC layer to that

representation, and we train it using the weighted cross-entropy loss. This version performed better than the original version adapted from [28]. We refer to this version DCPL_m.

Visio-Lingual Hubless (ViLHub): This is our visiolinguistic loss \mathcal{L}_h^{TrSm} in Eq. 5 (Sec. 4). We add this loss to the other models described above to test how it would affect the performance. We test this model with varying scales for the ViL-Hubless loss.

5.3 Word2vec & WordNet Based Evaluation

For the evaluation of the models, we propose some metrics based on Word2vec and wordnet embeddings. The main motivation for proposing such metrics is that we found that the ground truth was too harsh as a metric for this problem. There are many examples where there is more than one reasonable answer. We show how we reached this conclusion with a human subject experiment using baseline model.

Human Subjects Experiment Setup. We randomly selected 100 examples from Visual Genome dataset [30] and evaluated 5 hypotheses for each. Out of these 5 hypotheses, 1 was the Ground Truth (GT) and the other 4 were top predictions from [70] excluding GT. In this experiment we had 3 human subjects, who were asked to evaluate each hypothesis from a scale of 1 to 5, 1 being the worst and 5 the best. The human subjects were blind to which hypothesis was the ground truth and which were a prediction by the model [70]. Afterward we created a new ground truth from the majority voting of the 3 subjects on each example, we call this new ground truth Human-GT.

We then computed the precision and recall of each of the human subjects and the ground truth against the Human-GT and we show the recall in Fig 3; we did not observe a difference in precision which is provided in appendix B. If we look at Fig 3 we can see that the ground truth has a very low recall compared with the human subjects. This implies that a very large percentage of the hypotheses labeled as incorrect by the ground truth is, in fact, correct (high number of false negatives). This confirms our suspicion that the GT on its own is not sufficient to gain a deep understanding of how the models are performing on this problem.

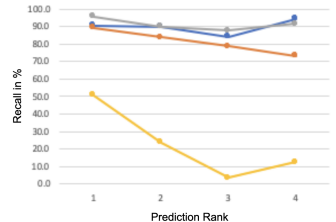


Fig. 3: Recall scores of each of the human subjects (gray, blue, orange) and the ground truth (gold) against the Human-GT.

Proposed Word2Vec & WordNet Analysis. Given that there are often multiple good answers, we wondered if we can come up with some kind of soft matching method to give partial credit to answers that aren't in the ground truth but are close. Motivated by the human subjects experiment discussed above, we propose to perform analysis based on six wordnet [39] metrics that have been investigated/used in the literature: Leacock-Chodorow Similarity(LCH), Wu-Palmer Similarity(WUP), Resnik (RES), Lin (LIN), Jiang-Conrath (JCN),

and path similarity (PATH)¹. In addition to two word2vec metrics trained on Visual Genome (VG) and Google News (GN). For each test example, we start by producing the top 250 closest predictions and store the corresponding confidence. Then, we use each of these metrics to retrieve the top T closest labels in the list of 250 predicted labels according to the chosen metric and mark it as relevant (i.e., label 1) to the given example in addition to the ground truth. We mark the remaining labels as irrelevant (label 0). After that, we report the Average Precision (AP) at 1, 5, 20, and 50 on the system. What this analysis tool measures is the capability of the system to bring concepts that are close to the ground truth (according to the given language metric) up in the rank.

5.4 Results

In Table 1 we report the results on the subject, object, and relation parts of an $\langle S, P, O \rangle$ triplet. We evaluate the reported models across several frequency bands: many, medium, and few. We chose the frequencies for these bands based on how steep the classes frequency distribution is. We can see in Table 1 that adding the ViL-Hubless (ViLHub) loss to any of the compared models consistently improves their performance on the medium and few categories of classes. If we compare the Baseline [70] with and without ViL-Hub 100k in Table 1 we can see that the ViL-Hubless improved the performance around 6% for the sbj/obj medium category, around 5% for the sbj/obj few category, and around 4% for the relation medium category. Similarly, if we compare the weighted-cross entropy model (WCE) with the weighted cross entropy + ViL-Hubless model (WCE + ViL-Hub) in sbj/obj branch we will find that adding the ViL-Hubless improved around 3% in the medium category, around 2.5% in the few category, and shows similar improvements for in the rel column. We can also see similar patterns when comparing the Focal Loss model with and without ViL-Hubless loss.

Additionally, in Table 2 and 3 we evaluate the models on GQA and VG datasets using the overall and per-class accuracies (acc) and mean rank (mr), which is consistent with the Visual VRD literature on comparing methods. The per-class accuracy and mean rank are the more important metrics in our case because they show performance on the tail. We report results on the subject, object, and relation separately, and combined as a triplet score. Table 2 shows that adding our ViL-Hubless (ViLHub) loss improves the performance on the per-class metrics, without hurting the overall performance and sometimes even improving it. To summarize, the ViL Hubless loss improved the performance on the tail when added to any of the models tested, regardless of their differences. This is seen when comparing any of the following models from Table 2: Baseline, Focal Loss, and Weighted Cross-entropy, Decoupling with their counterparts after adding the ViL-Hubless loss: Baseline + ViL-Hubless, Focal Loss + ViL-Hubless, Weighted CE + ViL-Hubless, and DCPL + ViL-Hubless. Namely, we see that in all four cases adding the ViL-Hubless improves the performance on

¹ reference to the implementation we used of these six functions <http://www.nltk.org/howto/wordnet.html>

Table 1: Performance on GQA

Model	subj/obj				rel			
	many	medium	few	all	many	medium	few	all
Baseline [70]	70.5	36.2	3.5	51.9	50.7	5.5	0.2	49.7
Baseline + ViLHub 10k	70.3	38.7	4.9	52.7	49.8	9.5	0.3	48.9
Baseline + ViLHub 50k	69.8	41.4	7.6	53.5	49.0	8.4	0.2	48.1
Baseline + ViLHub 100k	69.9	41.9	8.8	53.8	48.8	7.2	0.1	47.9
FL [34]	68.8	38.5	4.9	51.7	50.4	4.6	0.0	49.4
FL + ViLHub20k	69.8	41.7	8.1	53.7	49.0	7.0	0.1	48.1
WCE	39.3	36.5	16.2	35.5	35.9	29.0	14.3	35.6
WCE + ViLHub	35.2	39.5	18.8	34.2	33.5	31.3	15.6	33.3
FC	71.6	26.9	0.1	49.5	50.0	0.0	0.0	49.0
DCPL _τ [28]	71.4	27.0	0.1	49.4	50.0	0.0	0.0	48.9
DCPL _m	61.0	34.1	4.4	45.9	46.7	17.9	0.4	46.0
DCPL _m + ViLHub100k	58.4	38.1	6.1	45.7	40.5	21.3	0.9	39.9

Table 2: Performance on GQA

Model	Overall						Per-class			
	subj/obj		rel		triplet	subj/obj		rel		
	acc	mr	acc	mr	acc	acc	mr	acc	mr	
Baseline [70]	51.9	14.6	49.7	1.0	14.7	8.5	165.8	3.0	72.2	
Baseline + ViLHub 10k	52.8	14.0	48.9	3.0	14.9	9.3	156.1	3.6	76.0	
Baseline + ViLHub 50k	53.6	13.0	48.1	5.3	15.2	10.7	136.2	3.3	77.3	
Baseline + ViLHub 100k	53.9	12.9	47.9	6.6	15.3	11.3	125.3	3.2	77.3	
FL [34]	51.8	15.0	49.4	1.1	14.5	9.3	169.6	2.7	73.5	
FL + ViLHub20k	53.8	13.6	48.1	5.1	15.3	11.0	144.3	3.1	80.4	
WCE	35.8	22.7	35.6	2.7	5.3	13.9	80.9	13.0	40.2	
WCE + ViLHub	34.6	20.6	33.3	5.2	4.7	15.7	73.2	13.6	39.6	
FC	49.4	47.7	48.9	1.7	13.4	6.1	604.6	1.5	141.6	
DCPL _τ [28]	49.3	48.1	48.9	1.7	13.3	6.1	606.6	1.5	141.1	
DCPL _m	45.9	25.8	46.0	1.5	11.1	8.2	355.0	4.7	108.3	
DCPL _m + ViLHub100k	45.8	24.5	39.9	3.7	9.5	9.3	336.7	5.2	66.7	

the tail classes while keeping or sometimes improving the performance on the head classes. A similar pattern can be observed for VG dataset in Table 3. Note that improvement on GQA is more apparent than on VG, since VG dataset is more challenging and has more than 5 times the number of objects and more than 7 times the number of relationships compared to GQA.

We observed that the subjects and objects perform better on the tail when using a large ViL-Hubless scale while the relations perform better when using a smaller scale. This is due to the number of classes being smaller in the relations than in the subjects/objects. In section 5.5, we show our proposed analysis metrics to alleviate the harshness of the exact match metrics we discussed here.

Table 3: Performance on Visual Genome

Model	Overall					Per-class			
	sbj/obj		rel	triplet	sbj/obj		rel		
	acc	mr	acc	mr	acc	acc	mr	acc	mr
Baseline [70]	47.4	53.6	54.0	20.5	14.2	4.2	502.7	0.7	414.1
Baseline + ViLHub 10K	48.2	53.7	52.8	22.0	14.5	4.4	502.0	0.9	417.5
Baseline + ViLHub 100K	49.5	49.0	51.3	34.4	15.4	5.4	455.0	0.8	445.6
WCE	40.0	47.6	23.8	29.9	5.3	7.5	238.0	4.1	250.6
WCE + ViLHub	38.8	49.0	23.4	29.4	5.0	8.0	228.5	3.92	235.7
FL [34]	45.3	62.3	50.3	25.4	12.0	4.8	575.3	0.7	475.4
FC	44.5	171.2	51.3	37.0	11.0	4.1	1334.1	0.5	660.0
DCPL _m [28]	43.1	128.0	42.6	30.5	9.5	3.3	1308.3	1.3	710.8

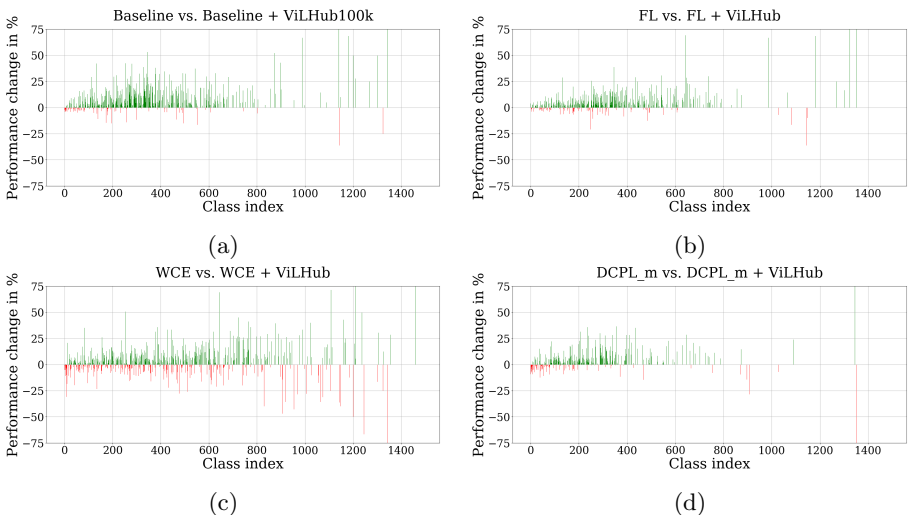


Fig. 4: **Comparisons of subject/object performance between models with and without ViL-Hubless.** We report the performance for all classes sorted by frequency. The head classes are on the left part of each plot while the tail classes are on the right. This figure clearly shows the performance gains on head and tail classes resulting from adding the ViL-Hubless loss to each of the models.

5.5 Analysis

In this section, we delve deeper into the improvements observed in Table 2 and analyze them more deeply to gain a better understanding of where the improvements in performance came from. Figure 4 shows several head-to-head comparisons between the most prominent of our performing models with and without using the ViL-Hubless loss. These comparisons between the models are done using synsets matching with the ground truth, which less harsh than the

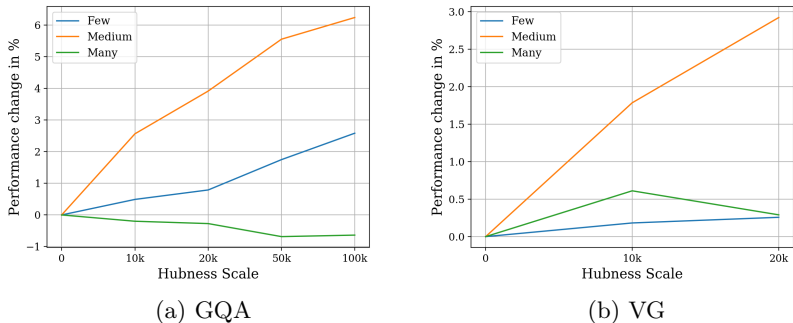


Fig. 5: **Performance changes on the many, medium, few parts of the classes as we increase the ViL-Hubless scale.** Many: most frequent 5% of classes, Medium: 30% to 5% most frequent, Few: least frequent 70% of classes. We can see that as we increase the ViL-Hubless scale, the performance improves on the medium and few classes (tail).

exact matching as it compares meaning instead of exact words. For example, if GT is car and prediction is vehicle, the exact matching would consider it as false while synset matching would consider it correct. This gives us a more fair comparison between the models’ performance. Figures 4a shows the difference in performance between using the baseline [70] on its own and using it along with the ViL-Hubless loss, here 462 classes improved, 106 worsened, and 918 stayed the same. Fig 4b compares the performance of the focal loss with and without adding the ViL-Hubless loss 411 classes improved, 119 worsened, and 956 didn’t change. Fig 4c compares the weighted cross entropy model with and without ViL-Hubless. Adding the ViL-Hubless improved 452 classes, worsened 285, and didn’t affect 749 classes Fig 4d compares using the decoupling method [28] with and without ViL-Hubless loss, which improved 299, worsened 93, and didn’t affect 1094 classes. The green bars indicate classes that improved due adding the ViL-Hubless and the red bars are classes that worsened. The height of the bars indicate the magnitude of improvement/worsening. The improvement on the y-axis is the absolute improvement of the classes in percentage accuracy. All figures show a clear improvement caused by adding the ViL-Hubless loss. This demonstrates how adding the ViL-Hubless loss to each of the models improves the performances of the classes across the frequency spectrum. We can see that on average the ViL-Hubless improves many more classes than it worsens and it improves more classes on the tail, which is the goal. This strongly establishes our point that adding the ViL-Hubless loss as a regularizer in long-tail problems pushes the models to learn classes across the spectrum, and prevents the models from solely focusing on improving the head classes.

To confirm that the ViL-Hubless loss was the cause of the improvements, we trained several models with varying scales for the ViL-Hubless loss with a scale of 0. Note that no ViL-Hubless loss is used which is equivalent to the Baseline

model explained in 5.2. Fig 5 shows how the performance increases on each of the medium, and few classes as we increase the ViL-Hubless scale. This further proves that the performance gains observed from adding the ViL-Hubless were indeed a result of improving the performance on the tail.

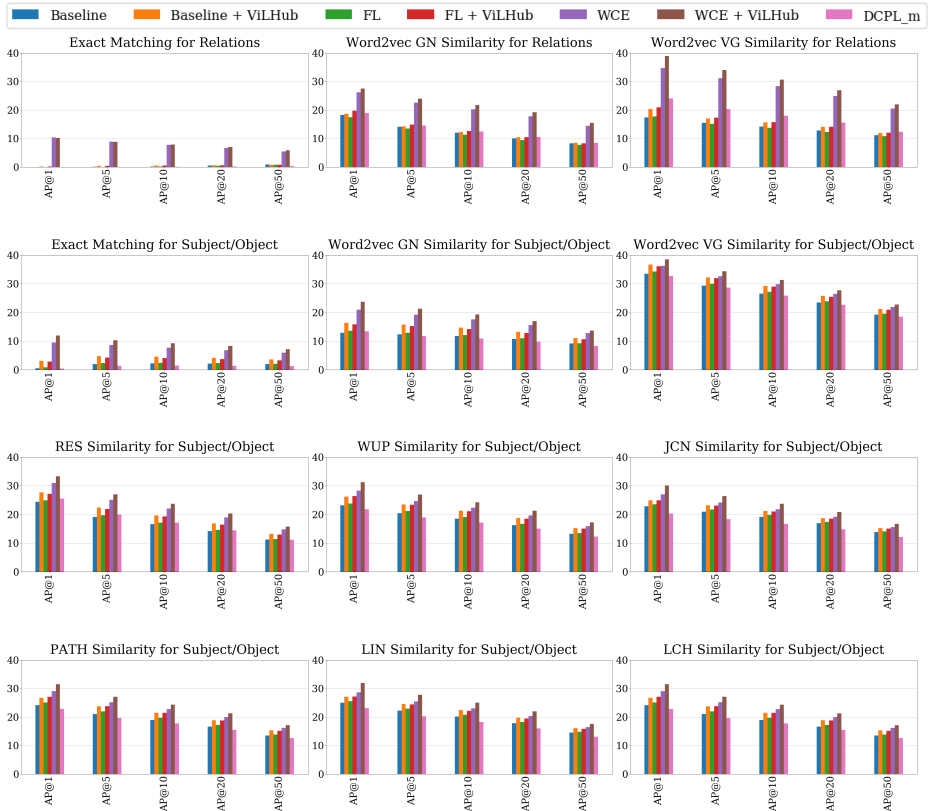


Fig. 6: Average precision analysis on the tail classes using a variety of metrics. We visualize results using exact similarity metrics, Word2Vec trained on Google News (GN) and Visual Genome (VG), Leacock-Chodorow (LCH), Wu-Palmer (WUP), Resnik (RES), Path, Lin, and Jiang-Conrath (JCN) similarity metrics. The models using ViL-Hubless show consistently superior performance on the tail, when compared to similar models without the ViL-Hubless.

Fig 6 shows the average precision of our model for the tail classes (least frequent 70%), following the protocol explained in 5.3. Concretely, in Fig 6 we use metrics to measure which models bring classes with similar meaning to the ground truth higher in the prediction rank. The results shown reveal that all models are doing significantly better than the harsh metric (exact matching)

implies. This agrees with our observations when evaluating qualitative examples from all the models and suggests that using the exact ground truth matching is too harsh and to some extent can be suboptimal. Another takeaway from this analysis is that similarity metrics trained on relevant data are better at evaluating the models' performances than metrics trained on less relevant data. This can be seen when comparing the Word2vec VG similarity metric (trained on VG) with the other metrics. Word2vec VG has higher scores than word2vec trained on Google News and wordNet metrics. Last, Fig 6 shows a consistent improvement for models using the ViL-Hubless loss. Overall, these results imply that our models are better at bringing semantically relevant concepts higher in the rank. Similar findings for the head classes are provided in the appendix D.

6 Conclusion

In this work, we proposed the study of a key problem for modern visual systems involving the generalization of visual relationship recognition to the tail of the underlying distribution. As seen from our extensive evaluation the problem we propose is particularly hard for a number of viable (and often, SOTA) alternatives. We showed that our novel adaptation of the hubless triplet softmax loss improves performance, especially for the least frequent classes, while maintaining and sometimes improving performance on the head classes. It will be an interesting future direction to investigate how one can further improve generalization on the tail by exploiting other meta-information of the underlying data, such as exploiting the shared part-based composition of common objects or using other forms of knowledge-transfer from the head classes to the tail.

References

1. Bengio, S.: The battle against the long tail (2011) 4
2. Bertinetto, L., Henriques, J.F., Valmadre, J., Torr, P., Vedaldi, A.: Learning feed-forward one-shot learners. In: Advances in Neural Information Processing Systems. pp. 523–531 (2016) 4
3. Blei, D.M., Ng, A.Y., Jordan, M.I.: Latent dirichlet allocation. *Journal of machine Learning research* **3**(Jan), 993–1022 (2003) 6
4. Brown, P.F., deSouza, P.V., Mercer, R.L., Pietra, V.J.D., Lai, J.C.: Class-based n-gram models of natural language. *Comput. Linguist.* **18**(4), 467479 (Dec 1992) 4
5. Chaudhry, A., Ranzato, M., Rohrbach, M., Elhoseiny, M.: Efficient lifelong learning with a-gem. In: ICLR (2019) 3
6. Chen, S.F., Goodman, J.: An empirical study of smoothing techniques for language modeling. *Computer Speech & Language* **13**(4), 359 – 394 (1999). <https://doi.org/https://doi.org/10.1006/csla.1999.0128>, <http://www.sciencedirect.com/science/article/pii/S0885230899901286> 4
7. Church, K.W., Hanks, P.: Word association norms, mutual information, and lexicography. *Comput. Linguist.* **16**(1), 2229 (Mar 1990) 4

8. Deng, J., Dong, W., Socher, R., Li, L.J., Li, K., Fei-Fei, L.: Imagenet: A large-scale hierarchical image database. In: Computer Vision and Pattern Recognition, 2009. CVPR 2009. IEEE Conference on. pp. 248–255. Ieee (2009) **1**
9. Dinu, G., Lazaridou, A., Baroni, M.: Improving zero-shot learning by mitigating the hubness problem. arXiv preprint arXiv:1412.6568 (2014) **5, 6**
10. Dong, Q., Gong, S., Zhu, X.: Class rectification hard mining for imbalanced deep learning. In: Proceedings of the IEEE International Conference on Computer Vision. pp. 1851–1860 (2017) **4**
11. Elhoseiny, M., Elfeki, M.: Creativity inspired zero-shot learning. In: ICCV (2019) **2**
12. Elhoseiny, M., Elgammal, A., Saleh, B.: Write a classifier: Predicting visual classifiers from unstructured text. IEEE transactions on pattern analysis and machine intelligence **39**(12), 2539–2553 (2017) **2, 3**
13. Elhoseiny, M., Liu, J., Cheng, H., Sawhney, H., Elgammal, A.: Zero-shot event detection by multimodal distributional semantic embedding of videos. In: AAAI (2016) **2**
14. Elhoseiny, M., Saleh, B., Elgammal, A.: Write a classifier: Zero-shot learning using purely textual descriptions. In: Proceedings of the IEEE International Conference on Computer Vision. pp. 2584–2591 (2013) **3**
15. Faghri, F., Fleet, D.J., Kiros, J.R., Fidler, S.: Vse++: Improving visual-semantic embeddings with hard negatives. In: Proceedings of the British Machine Vision Conference (BMVC) (2018), <https://github.com/fartashf/vsepp> **3, 6, 7**
16. Finn, C., Abbeel, P., Levine, S.: Model-agnostic meta-learning for fast adaptation of deep networks. In: Proceedings of the 34th International Conference on Machine Learning-Volume 70. pp. 1126–1135. JMLR. org (2017) **4**
17. Frome, A., Corrado, G.S., Shlens, J., Bengio, S., Dean, J., Mikolov, T., et al.: Devise: A deep visual-semantic embedding model. In: Advances in neural information processing systems. pp. 2121–2129 (2013) **3, 6**
18. Gardis, S., Komodakis, N.: Dynamic few-shot visual learning without forgetting. In: Proceedings of the IEEE Conference on Computer Vision and Pattern Recognition. pp. 4367–4375 (2018) **4**
19. Gong, Y., Ke, Q., Isard, M., Lazebnik, S.: A multi-view embedding space for modeling internet images, tags, and their semantics. International journal of computer vision **106**(2), 210–233 (2014) **3**
20. Good, I.J.: The population frequencies of species and the estimation of population parameters. Biometrika **40**(3/4), 237–264 (1953), <http://www.jstor.org/stable/2333344> **4**
21. Ha, D., Dai, A., Le, Q.V.: Hypernetworks. arXiv preprint arXiv:1609.09106 (2016) **4**
22. He, K., Zhang, X., Ren, S., Sun, J.: Deep residual learning for image recognition. In: Proceedings of the IEEE conference on computer vision and pattern recognition. pp. 770–778 (2016) **1**
23. Huang, C., Li, Y., Change Loy, C., Tang, X.: Learning deep representation for imbalanced classification. In: Proceedings of the IEEE conference on computer vision and pattern recognition. pp. 5375–5384 (2016) **4**
24. Huang, G., Liu, Z., Van Der Maaten, L., Weinberger, K.Q.: Densely connected convolutional networks. In: Proceedings of the IEEE conference on computer vision and pattern recognition. pp. 4700–4708 (2017) **1**
25. Huang, J., Qiu, Q., Church, K.: Hubless nearest neighbor search for bilingual lexicon induction. In: Proceedings of the 57th Annual Meeting of the Association for Computational Linguistics. pp. 4072–4080 (2019) **2, 5, 6, 8**

26. Hudson, D.A., Manning, C.D.: Gqa: a new dataset for compositional question answering over real-world images. arXiv preprint arXiv:1902.09506 (2019) [3](#), [8](#)
27. Johnson, J., Karpathy, A., Fei-Fei, L.: Denscap: Fully convolutional localization networks for dense captioning. In: Proceedings of the IEEE Conference on Computer Vision and Pattern Recognition (2016) [9](#)
28. Kang, B., Xie, S., Rohrbach, M., Yan, Z., Gordo, A., Feng, J., Kalantidis, Y.: Decoupling representation and classifier for long-tailed recognition. In: International Conference on Learning Representations (2020), <https://openreview.net/forum?id=r1gRTCVFvB> [4](#), [9](#), [10](#), [12](#), [13](#), [14](#), [23](#), [24](#)
29. Kiros, R., Salakhutdinov, R., Zemel, R.: Multimodal neural language models. In: International Conference on Machine Learning. pp. 595–603 (2014) [3](#), [7](#)
30. Krishna, R., Zhu, Y., Groth, O., Johnson, J., Hata, K., Kravitz, J., Chen, S., Kalantidis, Y., Li, L.J., Shamma, D.A., et al.: Visual genome: Connecting language and vision using crowdsourced dense image annotations. International Journal of Computer Vision **123**(1), 32–73 (2017) [8](#), [9](#), [10](#)
31. Krizhevsky, A., Sutskever, I., Hinton, G.E.: Imagenet classification with deep convolutional neural networks. In: Advances in neural information processing systems. pp. 1097–1105 (2012) [1](#)
32. Lei Ba, J., Swersky, K., Fidler, S., et al.: Predicting deep zero-shot convolutional neural networks using textual descriptions. In: Proceedings of the IEEE International Conference on Computer Vision. pp. 4247–4255 (2015) [3](#)
33. Li, Y., Ouyang, W., Wang, X., Tang, X.: Vip-cnn: Visual phrase guided convolutional neural network. In: Computer Vision and Pattern Recognition (CVPR), 2017 IEEE Conference on. pp. 7244–7253. IEEE (2017) [3](#)
34. Lin, T.Y., Goyal, P., Girshick, R., He, K., Dollár, P.: Focal loss for dense object detection. In: Proceedings of the IEEE international conference on computer vision. pp. 2980–2988 (2017) [2](#), [3](#), [4](#), [8](#), [9](#), [12](#), [13](#), [23](#), [24](#)
35. Liu, Z., Luo, P., Wang, X., Tang, X.: Deep learning face attributes in the wild. In: Proceedings of the IEEE international conference on computer vision. pp. 3730–3738 (2015) [4](#)
36. Liu, Z., Miao, Z., Zhan, X., Wang, J., Gong, B., Yu, S.X.: Large-scale long-tailed recognition in an open world. In: Proceedings of the IEEE Conference on Computer Vision and Pattern Recognition. pp. 2537–2546 (2019) [2](#), [4](#)
37. Lu, C., Krishna, R., Bernstein, M., Fei-Fei, L.: Visual relationship detection with language priors. In: European Conference on Computer Vision. pp. 852–869. Springer (2016) [2](#), [3](#)
38. Mikolov, T., Sutskever, I., Chen, K., Corrado, G.S., Dean, J.: Distributed representations of words and phrases and their compositionality. In: Advances in neural information processing systems. pp. 3111–3119 (2013) [5](#), [7](#), [9](#)
39. Miller, G.A.: Wordnet: a lexical database for english. Communications of the ACM (1995) [3](#), [10](#)
40. Norouzi, M., Mikolov, T., Bengio, S., Singer, Y., Shlens, J., Frome, A., Corrado, G., Dean, J.: Zero-shot learning by convex combination of semantic embeddings. In: International Conference on Learning Representations (2014), <http://arxiv.org/abs/1312.5650> [3](#), [6](#)
41. Oh Song, H., Xiang, Y., Jegelka, S., Savarese, S.: Deep metric learning via lifted structured feature embedding. In: Proceedings of the IEEE Conference on Computer Vision and Pattern Recognition. pp. 4004–4012 (2016) [4](#)
42. Ouyang, W., Wang, X., Zhang, C., Yang, X.: Factors in finetuning deep model for object detection with long-tail distribution. In: Proceedings of the IEEE conference on computer vision and pattern recognition. pp. 864–873 (2016) [4](#)

43. Pielou, E.: The measurement of diversity in different types of biological collections. *Journal of Theoretical Biology* **13**, 131 – 144 (1966). [https://doi.org/https://doi.org/10.1016/0022-5193\(66\)90013-0](https://doi.org/https://doi.org/10.1016/0022-5193(66)90013-0), <http://www.sciencedirect.com/science/article/pii/0022519366900130> **4**
44. Plummer, B.A., Mallya, A., Cervantes, C.M., Hockenmaier, J., Lazebnik, S.: Phrase localization and visual relationship detection with comprehensive image-language cues. In: 2017 IEEE International Conference on Computer Vision (ICCV). pp. 1946–1955. IEEE (2017) **2, 3, 6**
45. Qian, Q., Shang, L., Sun, B., Hu, J., Li, H., Jin, R.: Softtriple loss: Deep metric learning without triplet sampling. In: Proceedings of the IEEE International Conference on Computer Vision. pp. 6450–6458 (2019) **6**
46. Radovanović, M., Nanopoulos, A., Ivanović, M.: Hubs in space: Popular nearest neighbors in high-dimensional data. *Journal of Machine Learning Research* **11**(Sep), 2487–2531 (2010) **5, 6**
47. Ravi, S., Larochelle, H.: Optimization as a model for few-shot learning (2017) **4**
48. Ren, M., Liao, R., Fetaya, E., Zemel, R.S.: Incremental few-shot learning with attention attractor networks. arXiv preprint arXiv:1810.07218 (2018) **4**
49. Ren, M., Triantafillou, E., Ravi, S., Snell, J., Swersky, K., Tenenbaum, J.B., Larochelle, H., Zemel, R.S.: Meta-learning for semi-supervised few-shot classification. arXiv preprint arXiv:1803.00676 (2018) **2**
50. Russakovsky, O., Deng, J., Su, H., Krause, J., Satheesh, S., Ma, S., Huang, Z., Karpathy, A., Khosla, A., Bernstein, M., Berg, A.C., Fei-Fei, L.: Imagenet large scale visual recognition challenge (2014) **1**
51. Salakhutdinov, R., Torralba, A., Tenenbaum, J.: Learning to share visual appearance for multiclass object detection. In: Computer Vision and Pattern Recognition (CVPR), 2011 IEEE Conference on. pp. 1481–1488. IEEE (2011) **2, 4**
52. Santoro, A., Bartunov, S., Botvinick, M., Wierstra, D., Lillicrap, T.: Meta-learning with memory-augmented neural networks. In: International conference on machine learning. pp. 1842–1850 (2016) **4**
53. Schmidhuber, J.: A neural network that embeds its own meta-levels. In: IEEE International Conference on Neural Networks. pp. 407–412. IEEE (1993) **4**
54. Simon, H.A.: On a class of skew distribution functions. *Biometrika* **42**(3/4), 425–440 (1955), <http://www.jstor.org/stable/2333389> **4**
55. Simonyan, K., Zisserman, A.: Very deep convolutional networks for large-scale image recognition. In: ICLR (2015) **1**
56. Smith, S.L., Turban, D.H., Hamblin, S., Hammerla, N.Y.: Offline bilingual word vectors, orthogonal transformations and the inverted softmax. In: ICLR (2017) **5, 6**
57. Snell, J., Swersky, K., Zemel, R.: Prototypical networks for few-shot learning. In: Advances in Neural Information Processing Systems. pp. 4077–4087 (2017) **2**
58. Socher, R., Ganjoo, M., Manning, C.D., Ng, A.: Zero-shot learning through cross-modal transfer. In: Advances in neural information processing systems. pp. 935–943 (2013) **3**
59. Sung, F., Yang, Y., Zhang, L., Xiang, T., Torr, P.H., Hospedales, T.M.: Learning to compare: Relation network for few-shot learning. In: Proceedings of the IEEE Conference on Computer Vision and Pattern Recognition. pp. 1199–1208 (2018) **4**
60. Vendrov, I., Kiros, R., Fidler, S., Urtasun, R.: Order-embeddings of images and language. arXiv preprint arXiv:1511.06361 (2015) **3, 7**

61. Wang, L., Li, Y., Lazebnik, S.: Learning deep structure-preserving image-text embeddings. In: Proceedings of the IEEE conference on computer vision and pattern recognition. pp. 5005–5013 (2016) [3](#)
62. Wang, Y.X., Ramanan, D., Hebert, M.: Learning to model the tail. In: Advances in Neural Information Processing Systems. pp. 7029–7039 (2017) [2](#), [4](#)
63. Xian, Y., Lampert, C.H., Schiele, B., Akata, Z.: Zero-shot learning-a comprehensive evaluation of the good, the bad and the ugly. PAMI (2018) [2](#)
64. Xian, Y., Lampert, C.H., Schiele, B., Akata, Z.: Zero-shot learning-a comprehensive evaluation of the good, the bad and the ugly. IEEE transactions on pattern analysis and machine intelligence (2018) [3](#)
65. Xian, Y., Lorenz, T., Schiele, B., Akata, Z.: Feature generating networks for zero-shot learning. In: CVPR (2018) [2](#)
66. Xu, D., Zhu, Y., Choy, C.B., Fei-Fei, L.: Scene graph generation by iterative message passing. In: Proceedings of the IEEE Conference on Computer Vision and Pattern Recognition. vol. 2 (2017) [3](#)
67. Yu, R., Li, A., Morariu, V.I., Davis, L.S.: Visual relationship detection with internal and external linguistic knowledge distillation. In: The IEEE International Conference on Computer Vision (ICCV) (2017) [3](#)
68. Zhang, H., Kyaw, Z., Chang, S.F., Chua, T.S.: Visual translation embedding network for visual relation detection. In: Computer Vision and Pattern Recognition (CVPR), 2017 IEEE Conference on. pp. 3107–3115. IEEE (2017) [3](#)
69. Zhang, J., Elhoseiny, M., Cohen, S., Chang, W., Elgammal, A.: Relationship proposal networks. In: Proceedings of the IEEE Conference on Computer Vision and Pattern Recognition. pp. 5678–5686 (2017) [2](#)
70. Zhang, J., Kalantidis, Y., Rohrbach, M., Paluri, M., Elgammal, A., Elhoseiny, M.: Large-scale visual relationship understanding. In: Proceedings of the AAAI Conference on Artificial Intelligence. vol. 33, pp. 9185–9194 (2019) [3](#), [6](#), [7](#), [8](#), [9](#), [10](#), [11](#), [12](#), [13](#), [14](#), [23](#), [24](#)
71. Zhang, R., Che, T., Ghahramani, Z., Bengio, Y., Song, Y.: Metagan: An adversarial approach to few-shot learning. In: Advances in Neural Information Processing Systems. pp. 2365–2374 (2018) [2](#)
72. Zhang, X., Fang, Z., Wen, Y., Li, Z., Qiao, Y.: Range loss for deep face recognition with long-tailed training data. In: Proceedings of the IEEE International Conference on Computer Vision. pp. 5409–5418 (2017) [4](#)
73. Zhu, X., Anguelov, D., Ramanan, D.: Capturing long-tail distributions of object subcategories. In: Proceedings of the IEEE Conference on Computer Vision and Pattern Recognition. pp. 915–922 (2014) [4](#)
74. Zhu, X., Vondrick, C., Fowlkes, C.C., Ramanan, D.: Do we need more training data? International Journal of Computer Vision **119**(1), 76–92 (2016) [4](#)
75. Zhuang, B., Liu, L., Shen, C., Reid, I.: Towards context-aware interaction recognition for visual relationship detection. In: The IEEE International Conference on Computer Vision (ICCV) (Oct 2017) [3](#)
76. Zipf, G.K.: The psycho biology of language an introduction to dynamic philology. (1935) [2](#)
77. Zipf, G.K.: Human behavior and the principle of least effort. (1949) [2](#)

A Qualitative Examples

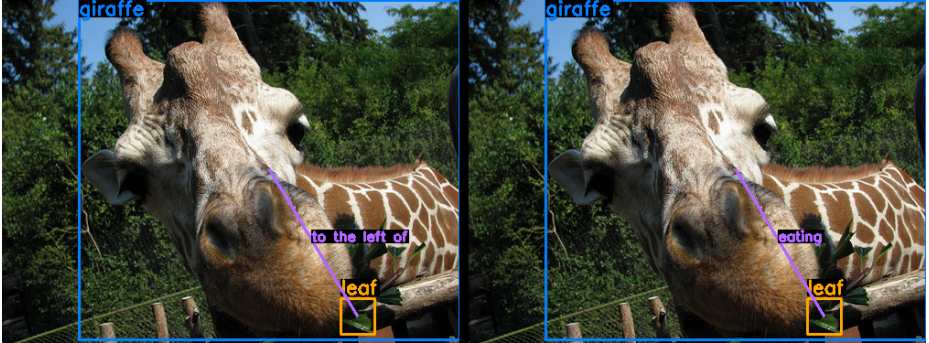


Fig. 7: A qualitative example showing how the model with the ViL-Hubless loss performs better on tail relation classes. Blue is subject, purple is relation, and orange is object. The left image is the Baseline model, and the right image is Baseline + ViLHub model



Fig. 8: A qualitative example showing how the model with the ViL-Hubless loss performs better on tail subject/object classes. Left image is the Baseline model, and right image is Baseline + ViLHub model

Fig 7 shows an example of one of the cases where the Baseline model (left image) predicts a head class *to the left of* that doesn't fit well while the Baseline + ViL-Hubless model (right image) instead predicts a tail class *eating* that is more accurate and descriptive in this case. Fig 8 shows a similar example where the Baseline predicts class *roof* for the subject, which is not wrong, but the Baseline + ViLHub model predicts a more specific and descriptive class in this which is *dome*. More qualitative examples can be found in the attached video.

B Motivation For Word2Vec and Wordnet Metrics

The ground truth by construction assumes that there is one and only one right answer. Fig 9 shows an example of such case. In this case, the top 5 predictions from the model are all correct and very plausible. It’s very hard to say any of these are wrong. This illustrates that the gold standard with one correct answer only is fundamentally flawed for this task, and this is the motivation behind our proposed metrics.



Fig. 9: **This example is meant to show how some boxes can have multiple good answers.** The top 5 predictions for the above box are: [Baseball Cap, Cap, Green Hat, Hat, Head]. This shows how it is unreasonable to evaluate this task assuming there is only one correct answer.

Fig 10 shows the precision curve between the human subjects and the ground truth when evaluated against the Human-GT defined in the paper. We can see that the precision scores for human subjects and GT are close to each other when compared with the recall scores shown in the paper. What this implies is that the labels that GT labels as correct are also considered correct by the Human-GT (low number of false positives).

C Additional Results

We showed that the GT is not sufficient on its own to evaluate a model’s performance, so calculated the metrics using synset matching. This means that if the wordnet synset of the prediction matches the wordnet synset of the GT this counts as a correct prediction. We show the metrics calculated using this approach in table 4. We can see that the same pattern of adding ViL-Hubless Loss

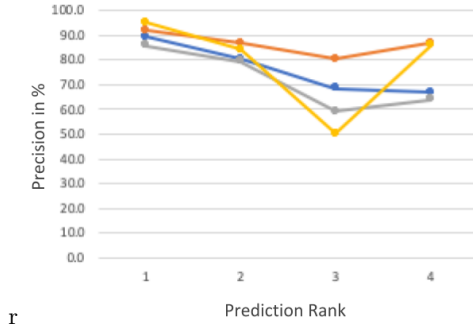


Fig. 10: Precision scores of each of the human subjects (gray, blue, red) and the ground truth (gold) against the Human-GT

Table 4: Performance on GQA with Synset Matching

Model	subj/obj				rel			
	many	medium	few	all	many	medium	few	all
Baseline [70]	73.0	42.4	11.6	56.2	96.5	15.5	8.1	94.7
Baseline + ViLHub 10k	72.9	45.0	13.2	57.1	94.4	18.6	8.1	92.7
Baseline + ViLHub 50k	72.6	47.6	16.1	58.0	93.4	17.3	8.0	91.7
Baseline + ViLHub 100k	72.6	48.2	17.3	58.4	92.8	16.3	7.9	91.1
FL [34]	71.9	44.8	13.2	56.5	96.4	15.1	8.2	94.6
FL + ViLHub20k	72.5	48.0	16.7	58.2	93.4	15.9	8.2	91.7
WCE	47.6	44.3	22.9	43.4	72.6	34.0	22.1	71.7
WCE + ViLHub	43.9	46.9	25.5	42.3	69.1	37.0	23.8	68.3
FC	74.1	32.7	7.1	53.5	96.1	9.0	6.4	94.3
DCPL _r [28]	73.9	32.7	7.0	53.4	96.2	9.1	6.2	94.3
DCPL _m [28]	65.0	40.1	11.4	50.9	89.3	24.9	9.1	87.8
DCPL _m + ViLHub100k	62.3	44.3	13.6	50.8	78.7	27.8	9.2	77.5

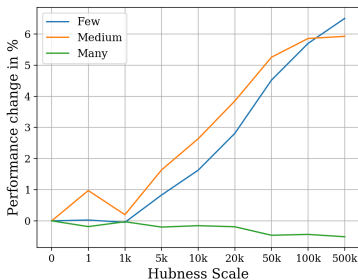
Table 5: Per-class word similarity on subjects/objects in GQA

Models	lch	wup	lin	path	w2v
Baseline [70]	51.2	59.4	36.8	27.5	45.2
Baseline + ViLHub 10k	52.0	60.1	37.8	28.6	45.8
Baseline + ViLHub 50k	53.1	61.0	39.0	30.1	46.7
Baseline + ViLHub 100k	53.4	61.3	39.5	30.6	47.1
FL [34]	51.8	60.0	37.5	28.3	45.7
FL + ViLHub20k	53.2	61.1	39.1	30.3	47.0
WCE	53.5	61.1	39.4	31.8	47.8
WCE + ViLHub	54.8	62.1	41.0	33.5	49.2
FC	48.9	57.1	33.8	24.5	43.3
DCPL _r [28]	49.0	57.3	33.9	24.5	43.2
DCPL _m [28]	49.1	57.4	34.1	25.8	43.0
DCPL _m + ViLHub100k	50.4	58.4	35.5	27.3	44.7

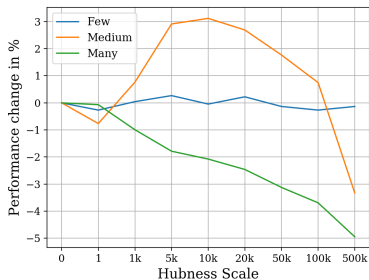
improves performance on the medium and few classes but with higher numbers overall for all the models.

Table 6: Performance on VG

	sbj/obj				rel			
	many	medium	few	all	many	medium	few	all
Baseline [70]	65.5	16.6	0.3	46.8	58.9	1.8	0.0	54.0
Baseline + ViLHub 10K	66.2	18.4	0.4	47.6	57.6	2.0	0.0	52.8
Baseline + ViLHub 100K	65.7	24.2	1.3	48.4	56.0	0.2	0.0	51.3
WCE	46.7	29.7	5.4	37.3	25.1	16.7	3.3	23.8
WCE + ViLHub	44.3	30.3	6.1	36.0	24.6	16.5	3.3	23.4
FL [34]	59.8	22.7	0.8	44.2	54.9	1.1	0.0	50.3
FC	68.1	13.2	0.0	43.1	57.7	0.0	0.0	51.3
DCPL _m [28]	60.9	9.6	0.0	42.4	46.4	2.3	0.0	42.6



(a) Trend on subjects/objects



(b) Trend on relations

Fig. 11: This is a similar version to the figures shown in the main paper, tested with more ViL-Hubless scales. The figure shows how the performance changes on the many, medium, few parts of the classes as we increase the ViL-Hubless scale. Many: most frequent 5% of classes, Medium: 20% to 5% most frequent, Few: least frequent 80% of classes

In Table 5 shows the average per-class word similarity measured through wordnet and word2vec metrics for the subject and object categories. We can see the pattern more consistently here, where the models with the ViL-Hubless loss added have higher average per-class word similarity to the ground truth. Table 6 shows a similar patterns to the table in the main paper. Adding the ViLHub loss seems to improve performance on tail classes, without hurting the head performance and sometimes improving it. It seems that the higher the number of classes the higher the hubness scale needed, this is observed from how the relationships benefit from small hubness scale while the subjects and objects benefit much more from high hubness scales. This is explored further in Fig 5

D Further Analysis

From Fig 5 we can see that as we increase the ViL-Hubless scale, the performance improves on the medium and few classes (tail) for subjects and objects. However

for the relations, the optimal ViL-Hubless scale seems to lie somewhere around 10k, if we increase the scale further the performance starts to drop significantly. More experimentation is needed to determine the exact optimal value for ViLHub scale for subjects/objects and relations.

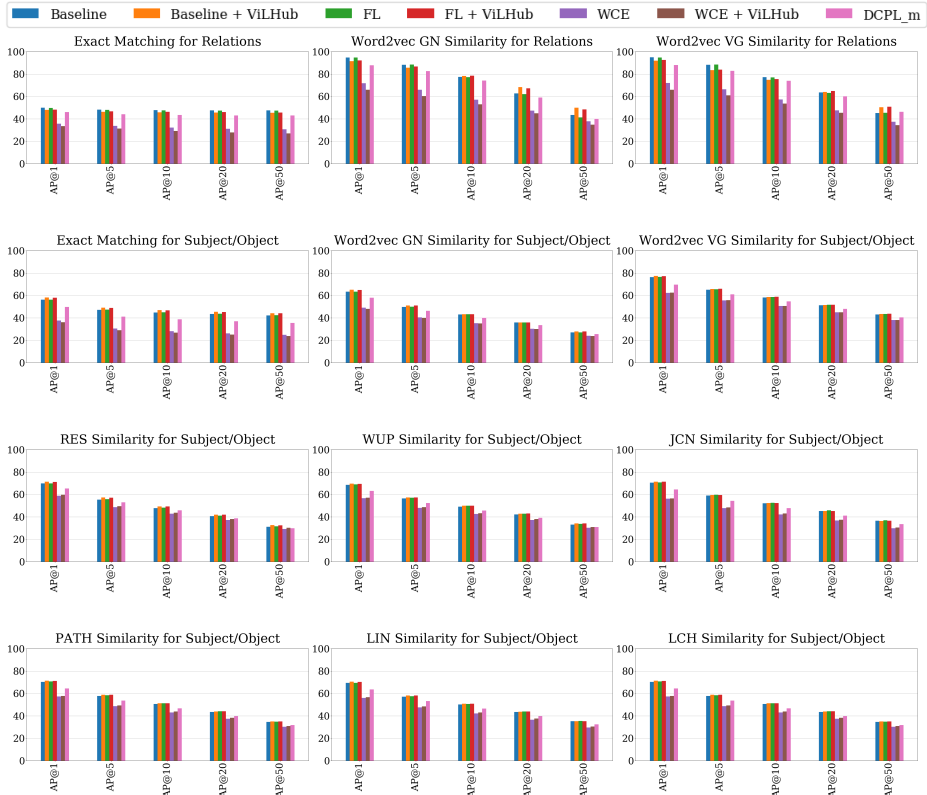


Fig.12: Average precision analysis on the head classes using exact metrics, Word2Vec trained on Google News (GN) and Visual Genome (VG), Leacock-Chodorow, Wu-Palmer (WUP), Resnik (RES), Path, Lin, and Jiang-Conrath (JCN) similarity metrics.

Figures 12 show the same analysis done in the main paper section 5.5 Table 6 but repeated for the head (top 30% of classes).